

A Topologically Complete Theory of Weaving

ERGUN AKLEMAN* JIANER CHEN† SHIYU HU‡ JONATHAN L. GROSS§

Abstract

Recent advances in the computer graphics of woven images on arbitrary surfaces in 3-space motivate the development of weavings for higher genus surfaces. Our paradigm differs markedly from what Grünbaum and Shepard have provided for the plane. In particular, we demonstrate herein how weavings on surfaces in 3-space are inducible from graph imbeddings on surfaces in 3-space. Moreover, we show that the two most frequently invoked subdivision algorithms in computer graphics, the Catmull-Clark and Doo-Sabin algorithms, correspond nicely to topological surgery operations on the induced weavings. A considerable advantage of our model is that it is topological. This permits the graphic designer to superimpose strand colors and geometric attributes — distances, angles, and curvatures — that conform to manufacturing or artistic criteria.

Version: 15:31 March 1, 2012

1 Introduction

Woven objects, including fabrics, cloths, sweaters, and baskets, can be rich and beautiful, and they are interesting in art, mathematics, and manufacturing. From a topological perspective, a (cyclic) *weaving* is simply an immersion (i.e., with overcrossings and undercrossings) of a link (i.e., a collection of linked knots) on a surface in 3-space. For instance, most familiar Celtic knot patterns [9] are weavings on the plane.

A recently developed method for modeling weavings on an arbitrary topological surface is based on *extended graph rotation systems* [3, 7]. If we imagine each face-boundary walk (abbr. *fb-walk*) of a graph imbedding $\pi : G \rightarrow S$ to be lying slightly inside the face, then the fb-walks form a collection of disjoint cycles on the orientable surface S . Each edge e of the graph G induces two parallel line-segments (see Figure 1a), which may occur either on two disjoint fb-walks or both on the same fb-walk. The operation of *twisting the edge* e involves first cutting both line-segments near the same end of e (as in Figure 1b), next crossing one segment over the other (as in Figure 1c), and finally splicing the ends of the segments (as in Figure 1d).

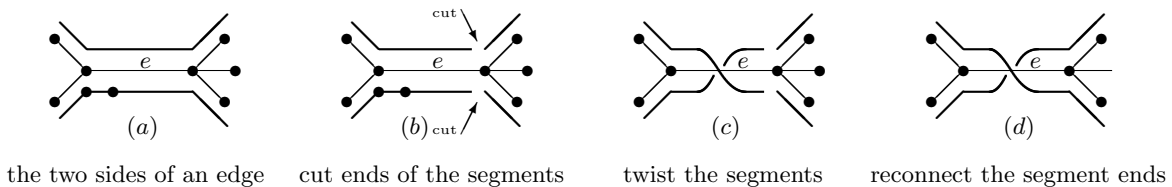


Figure 1: Twisting the two sides of an edge

There is a major conceptual difference here from the standard approach to graph imbeddings. In standard topological graph theory (see [15]), twisting an edge means changing the local orientation along

*Supported in part by NSF Grant CCF-0917288, Visualization Department, Texas A&M University, College Station, TX 77843, USA. Email: ergun@viz.tamu.edu.

†Supported in part by NSF Grants CCF-0830455 and CCF-0917288, Department of Computer Science and Engineering, Texas A&M University, College Station, TX 77843, USA. Email: chen@cse.tamu.edu.

‡Supported in part by NSF Grant CCF-0917288, Department of Computer Science and Engineering, Texas A&M University, College Station, TX 77843, USA. Email: shiyu@cse.tamu.edu.

§Department of Computer Science, Columbia University, New York, NY 10027, USA. Email: gross@cs.columbia.edu.

the edge and changing the topology of the underlying surface. In our approach here, twisting an edge means introducing a crossing of *strands* on the same surface, but not changing the surface topology.

The correspondence between a graph imbedding $G \rightarrow S$ and an immersion of a collection of circuits is illustrated in Figure 2. The upper row depicts a planar graph (in (a)) without twisted edges, imbedded on the sphere (in (b)), where each edge is thickened to a band (in (c)), and with the sides of the bands forming a collection of disjoint cycles (in (d)) imbedded on the sphere. The lower row in Figure 2 depicts the same planar graph, this time with a set of twisted edges (in (a')), each marked with a cross) imbedded on the same sphere (in (b')), with the twisted edges regarded as twisted strip bands (in (c')), and lastly with the sides of the bands forming a collection of cycles (in (d')) immersed on the sphere.

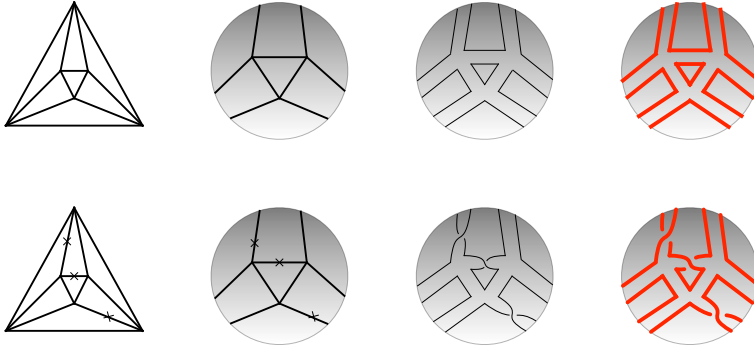


Figure 2: The correspondence between an imbedded graph and the induced weaving.

We have developed a graphics system [7], based on this framework, which offers these properties:

1. *Topological completeness*: the system can produce visual woven images on any closed surface in 3-space;
2. *Operational robustness*: all of the operations in our graphics system correspond to authentic topological operations, which provide secure control over the result of applying these operations, including certainty that the result is the intended topological object;
3. *Conciseness*: the graph imbedding and edge-twistings used to specify a weaving can be given by any of the extensively studied representations for graph imbeddings;
4. *Flexibility*: many dynamic surgery computer-graphics operations on weavings now can be implemented via their theoretical counterparts on the corresponding graph imbeddings. The latter have been extensively studied in the graph theory literature.

Figure 3 shows some woven images that have been created using our graphics system [7].

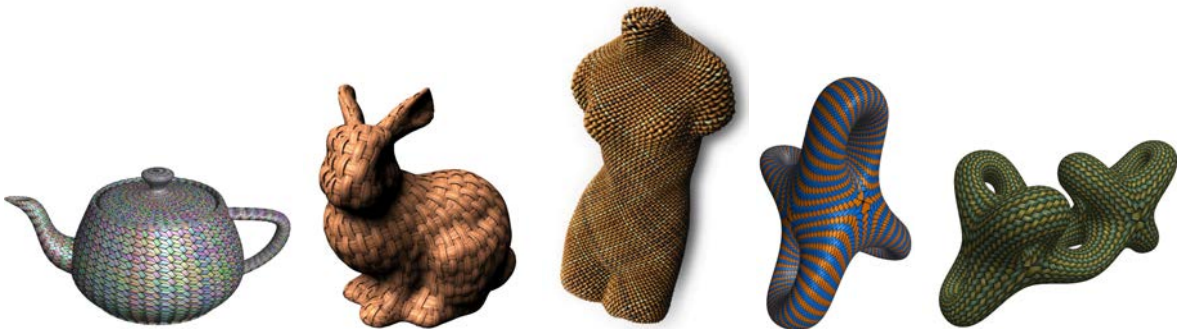


Figure 3: Examples of weavings on orientable surfaces

We observe that the bunny and Venus are woven on a simply connected surface, i.e., topologically equivalent to the sphere. However, the teapot and the two multi-toroidal surfaces at the right could not be specified within theories of weaving for the plane, such as that of Grünbaum and Shepard [17].

A full-fledged mathematical theory of weaving would provide answers to the following questions:

1. Given a weaving, what graph imbedding with twisted edges provides its specification?
2. How can we characterize the class of weavings that are inducible from graph imbeddings with marked twisted edges?
3. What are the relations between standard surgery operations on graph imbeddings and standard computer-graphics operations on the induced weavings?
4. How are edges of an imbedded graph twisted so that the induced weaving achieves certain specific weaving patterns?

This paper initiates a systematic study of these theoretical issues and others. We demonstrate here how our theoretical system, called an *extended rotation system* for a graph, models the familiar visual realities of woven objects. We identify the necessary and sufficient conditions for a graph imbedding with twisted edges to induce a valid weaving on a topological surface, and the necessary and sufficient conditions for a given weaving to be inducible from a graph imbedding.

In particular, we prove that all weavings on the plane are inducible from graph imbeddings. For instance, most Celtic weaves [9] correspond to planar graph imbeddings.

Moreover, we demonstrate the practicality of our theoretical system, by showing that the two most prevalent subdivision algorithms used in computer graphics, the Catmull-Clark method [10] and the Doo-Sabin method [12], correspond nicely to surgery operations on extended rotation systems. This will be important and critical to our construction of weavings in subsequent paper [4, 5, 6], where we derive properties and conditions for graph imbeddings to induce various well-known and beautiful weavings.

2 Background and Definitions

Our terminology here is consistent with standard textbooks on topological graph theory (e.g., [15]) and low-dimensional topology (e.g., [22]), but some augmentation is needed.

2.1 2-Manifolds and surfaces

A *2-manifold* is a compact topological space in which each point has a neighborhood homeomorphic to a closed disk. Its *boundary* is the set of points that do not have a neighborhood homeomorphic to an open disk; this is necessarily the union of a finite number of mutually disjoint closed curves. A connected 2-manifold is said to be *closed* if it has no boundary points; it is *orientable* if it does not contain a Möbius band. It is well-known that every orientable closed 2-manifold is homeomorphic to the boundary of a solid multi-toroidal object in Euclidean 3-space; the *genus of a 2-manifold* is the number of “handles” in such a solid object. The 2-manifold of genus i is denoted S_i .

A *surface* is either a 2-manifold or a connected topological space obtained from a 2-manifold by deleting some of its boundary components. Such a topological space is said to be *almost compact*. If S is a surface, then

- the surface $brc(S)$ is the result of restoring the missing boundary components;

the surface $brc(S)$ is called the *boundary-restored compactification* of S . By way of contrast,

- the surface $int(S)$ is the result of deleting all the boundary components;

it is called the *interior* of S . In what follows, a surface is taken to be orientable unless the alternative is declared or inferable from context. A cycle C on a surface S is *separating* if $S \setminus C$ is non-connected, and it is *contractible* if it bounds a disk on the surface S . Note that a contractible cycle is also a separating cycle.

2.2 Graph imbeddings and graph rotation systems

Our *graphs* are always undirected. They are connected except when explicit comment or context implies otherwise. Multi-edges and self-loops are allowed. A self-loop has only one endpoint, yet it has two distinguishable *edge-ends*. To distinguish between the two edge-ends of a self-loop, we regard the interior of each edge as parametrized by the open unit interval $(0, 1)$. The edge-ends are images of small neighborhoods of the limit points 0 and 1, respectively. This distinction permits us to differentiate between the two possible directions in which one can traverse any edge, including self-loops. Two different names can be given to the same endpoint of a self-loop, and interpreted, when context requires, as the two distinguishable edge-ends of the edge. For a multi-edge of multiplicity m , we can use m different names for one of their common endpoints and another m different names for the other endpoint. This allows distinct edges within a multi-edge to have distinguishable names. Under these conventions, each edge in the graph can be given as $e = [v, w]$, with two different ends v and w , and each edge induces two *oriented edges*, $\langle v, w \rangle$ and $\langle w, v \rangle$, each running from one edge-end of e to the other. A graph G is *k-regular* if every vertex in G is incident to exactly k edge-ends.

An *imbedding* $\iota : G \rightarrow S$ is a homeomorphism of the graph G onto a topological subspace of the surface S . The imbedding ι is *cellular* if every connected component of $S \setminus \iota(G)$, i.e., the interior of each *face* in the imbedding, is homeomorphic to an open disk.¹ Note that cellularity implicitly assumes that the graph G is connected.

Definition A *rotation* at a vertex v of a graph G is a cyclic ordering of the oriented edges originating at v . Often, when no ambiguity is created, we give the corresponding cyclic ordering of the other endpoints (i.e., other than v) of each of these oriented edges. A *pure rotation system* of the graph G consists of a set of rotations, one for each vertex of G . A *general rotation system* of G is a pure rotation system of G plus a subset of edges in G that are marked as “twisted”.

A *face corner* (sometimes, simply *corner*) in a rotation system ρ_G is a triple (v, e, e') , comprising a vertex v and two oriented edges e and e' oriented out of v , where the oriented edge e' immediately follows the oriented edge e in the rotation at v . The oriented edge e' is said to be *0-next* to the oriented edge e at v , and the oriented edge e is said to be *1-next* to the oriented edge e' at v .

It is easy to see that a cellular imbedding $\iota_0 : G \rightarrow S$ naturally induces a pure rotation system of the graph G . Also, note that every fb-walk in $\iota_0(G)$ is a closed walk, that is, a (cyclically ordered) sequence of oriented edges. Similarly, a cellular imbedding $\iota : G \rightarrow S$ of a graph G on a general (orientable or non-orientable) surface induces a general rotation system of the graph G . Conversely, it has been well-known since [18, 13] (for simple graphs) and [15] (for general graphs) that a general rotation system ρ_G of a graph G uniquely determines a cellular imbedding of G on a general (orientable or non-orientable) surface. In particular, if ρ_G is a pure rotation system, then the induced cellular imbedding is on an orientable surface. The surface S can be reconstructed from the rotation system ρ_G by first applying the *face-tracing algorithm* that constructs the fb-walks in ρ_G , and then matching the perimeter of a polygon to each fb-walk (see [15]); to an fb-walk of length s , we match an s -sided polygon. In the following discussion, we will interchangeably use the concepts of “a cellular imbedding of a graph” and “a pure rotation system of a graph”. In particular, it is perfectly meaningful to say “a pure rotation system of a graph on an orientable surface”.

¹Most studies of graph imbedding assume that the imbeddings are cellular. However, in the current paper, we do need to consider non-cellular graph imbeddings. Therefore, an “imbedding” in our discussion can be either cellular or non-cellular.

2.3 Weaving on topological surfaces

As in the topological literature [19], a continuous function σ from a collection \mathcal{C} of circuits to a surface S is an *immersion* if it is locally one-to-one, i.e., if for any point p in a cycle c in \mathcal{C} , there is a neighborhood N_p of p in the cycle c such that the function σ acts homeomorphically from N_p to $\sigma(N_p)$. Note that in the immersion σ , it is possible that the images of two circuits in \mathcal{C} intersect on S , or that the image of a single circuit in \mathcal{C} self-intersects on S . We regard the image of each circuit as a *strand* of the weaving. We may refer to the part of a strand between two specified crossings as a *segment* of that strand.

Our definition of immersions further requires that every intersection of the images of \mathcal{C} on S be a true intersection, rather than a tangency. The *thickness of a point* p on S under the immersion σ is the number of pre-images of p . The *thickness of the immersion* σ is the maximum thickness over all points on the surface S .

Our focus in the current paper is on weavings that are *cyclic*, that is, they are immersions of the union of a set of disjoint circuits on orientable surfaces.

Definition A *weaving* on a surface S is an immersion $\sigma : \mathcal{C} \rightarrow S$ of thickness at most 2, whose domain \mathcal{C} is a finite collection of circuits², in which there are only a finite number of points of thickness 2.

Definition A *gap in the weaving* $\sigma : \mathcal{C} \rightarrow S$ is a connected component of $S \setminus \sigma(\mathcal{C})$.

Definition A point of thickness 2 is called a *crossing*. A vertical order, called a *crossing-type*, is specified for the pre-images of each crossing to indicate which strand goes over the other at the crossing.

A weaving on a surface naturally induces a graph imbedded on the surface, which is defined as follows.

Definition Let $\sigma : \mathcal{C} \rightarrow S$ be a weaving on a surface S . If we regard each crossing in $\sigma(\mathcal{C})$ as a vertex, and each strand segment between two consecutive crossings as an edge, then we obtain a graph G_σ and an imbedding $\iota_\sigma : G_\sigma \rightarrow S$. The graph G_σ and the imbedding $\iota_\sigma : G_\sigma \rightarrow S$ are called the *σ -graph* and the *σ -imbedding*, respectively. If a strand has no crossings, then we give it a vertex v and make the strand a self-loop at v .

We remark that a σ -imbedding on a surface S_i need not be cellular. Moreover, the σ -graph need not be connected. For two weavings σ_1 and σ_2 on a surface S_i , if there is an auto-homeomorphism $h : S_i \rightarrow S_i$ that maps the imbedded σ_1 -graph to the imbedded σ_2 -graph, then by appropriately changing the crossing types, we can convert the weaving σ_1 to the weaving σ_2 .

2.4 The extended edge-twisting operation

Edge-twisting operations have been used extensively by topological graph theorists in the study of graph imbeddings on non-orientable surfaces. We now describe how the concept has been nicely borrowed and extended in computer graphics for the construction of weavings [7].

In a topological understanding of graph theory, traversing a twisted edge “reverses” the local orientation of the rotation system. Accordingly, a re-twisting of a twisted edge is equivalent to untwisting the edge, so the result of double-twisting an edge is topologically equivalent to no twisting at all. By way of contrast, in our model for weaving (see Figures 1 and 2), the two trace-pairs induced by an untwisted edge are regarded as two parallel segments of woven strands— and twisting the edge is interpreted as crossing the two strands. We are also interested in knowing which strand goes over and which strand under at a crossing point, and by how many turns a strand segment is twisted around the other segment. Double-twisting an edge is not the same as leaving it untwisted. Figure 4 gives some intuitive illustrations for edge-twisting in terms of the above interpretation.

²In this paper, both “cycles” and “circuits” refer to simple closed curves. The word “circuits” is used for the closed curves in the domain of a weaving, while the word “cycles” is used for general simple and closed curves, such as those on topological surfaces. The word “strand” is used for the image of a circuit in \mathcal{C} .

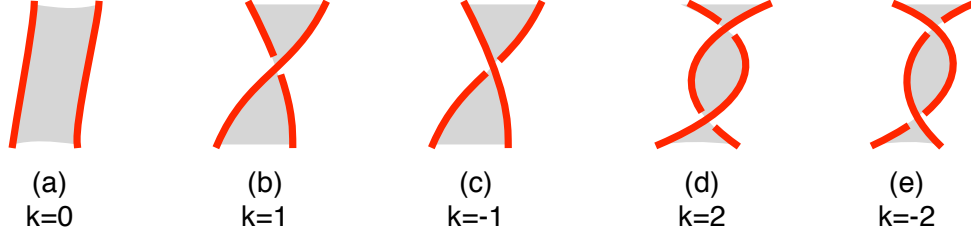


Figure 4: (a) an untwisted edge. (b) a counterclockwise twisted edge. (c) a clockwise twisted edge. (d) a double-counterclockwise twisted edge. (e) a double-clockwise twisted edge.

Comparing (b) with (c) and (d) with (e) in Figure 4 reveals that the direction in which we twist the edge is clearly relevant to which segment is over the other. This motivates the following definitions.

Definition An edge is 1^+ -*twisted* (resp. 1^- -*twisted*) if it is obtained from a flat paper strip, whose two sides are interpreted as the two parallel segments induced by the edge, by imagining yourself as positioned at one end of the strip, and twisting that end in counterclockwise (resp. clockwise) direction by 180° , while fixing the opposite end, assuming that you are facing the clock. There is an alternative characterization of a 1^+ -twisted edge may make it easier for some readers to visualize. As you walk along the corresponding flat strip, the edge to your left crosses over the edge to your right. We observe that this characterization is independent of the direction in which you traverse the strip.

See Figures 4(b,c) for an illustration. This concept can be naturally extended to multiple twists: we say that an edge is k^+ -*twisted* (resp. k^- -*twisted*) for an integer $k \geq 0$ if the edge can be obtained from an untwisted edge by k consecutive 1^+ -twists (resp. 1^- -twists). See Figures 4(d,e). In topological graph theory [15], a k^+ -twisted or k^- -twisted edge is equivalent to an untwisted edge if k is even, and equivalent to a normally twisted edge if k is odd.

Definition An *extended rotation system* (abbr. *ERS*) for a graph G is obtained from a pure rotation system of G by assigning a number k of twists, with $k \in \mathbb{Z}$, to every edge of G . (Elsewhere we have called this an “extended general rotation system”.)

Let ρ_G^0 be a pure rotation system of a graph G , which induces an imbedding $G \rightarrow S$. Assigning an edge-twist integer to every edge in G results in an ERS ρ_G of G . As explained above (see also Figures 1 and 2), the ERS ρ_G induces a weaving $\sigma : \mathcal{C} \rightarrow S$ on the surface S . Moreover, if we take evenly twisted edges as untwisted and oddly twisted edges as normally twisted, and if we let $\hat{\rho}_G$ denote the resulting (non-extended) general rotation system, then the classical *face-tracing algorithm* applied to the rotation system $\hat{\rho}_G$ produces a set of fb-walks [15].

It is easy to verify that these fb-walks of $\hat{\rho}_G$ are *exactly* the set of strands of the induced weaving σ . Also, based on the edge-twisting assignments in the ERS ρ_G , we can determine precisely which strand overcrosses and which undercrosses at each crossing, and how many times it crosses. Therefore, the face-tracing algorithm can be revised, with only small changes, to become a *strand-tracing algorithm* that produces all the strands of the induced weaving σ and provides complete information for the strand crossings.

For the convenience of our discussion, we present strand-tracing as Algorithm 1, where for an oriented edge $\langle u, w \rangle$ and $t \in \{0, 1\}$, $type(\langle u, w \rangle)$ is the twist-value assigned to the corresponding edge $[u, w]$, and the function $Next(\langle u, w \rangle, t)$ yields the oriented edge that is t -next to the oriented edge $\langle u, w \rangle$ at u . We say that a face corner (u, e, e') is “untraced” if no trace has followed the inverse of the oriented edge e while entering the vertex u , and then left u along the oriented edge e' .

Algorithm StrandTrace(ρ_G)Input: an ERS ρ_G for a graph G .Output: the set of strands for the weaving induced by ρ_G .

while there is an untraced face corner (u, e, e') in ρ_G **do**
 call Strand($\langle u, w \rangle, 0$). $\backslash\backslash$ assuming $e' = \langle u, w \rangle$

Subroutine Strand($\langle u_0, w_0 \rangle, t_0$) $\backslash\backslash \langle u_0, w_0 \rangle$ is an oriented edge, $t_0 \in \{0, 1\}$ is the “trace type”.

1. trace $\langle u_0, w_0 \rangle$; $t = t_0 + \text{type}([u_0, w_0]) \pmod{2}$;
2. $\langle u, w \rangle = \text{Next}(\langle w_0, u_0 \rangle, t)$; $\backslash\backslash u = w_0$
3. **while** $(\langle u, w \rangle \neq \langle u_0, w_0 \rangle)$ and $(t \neq t_0)$ **do**
 { trace $\langle u, w \rangle$; $t = t + \text{type}([u, w]) \pmod{2}$; $\langle u, w \rangle = \text{Next}(\langle w, u \rangle, t)$ }.

Algorithm 1: The strand-tracing algorithm.

3 Cellular Weavings

In this section, we derive a characterization of *cellular weavings* in terms of extended rotation systems on graphs.

Definition A weaving $\sigma : \mathcal{C} \rightarrow S$ is **cellular** if every gap in σ is homeomorphic to an open disk.

A woven object would look quite strange if unwoven patches of structural surface bulged out of the weave or if the weave could be pulled apart without tearing it. Theorem 3.1 (which is routine for topological graph theorists) explains that cellular weavings avoid such undesirable properties.

Theorem 3.1 *Let $\sigma : \mathcal{C} \rightarrow S_i$ be a non-cellular weaving. Then either there is a separating cycle in the surface S that separates σ into two disjoint non-empty weavings, or the weaving σ can be implemented as an immersion $\sigma : \mathcal{C} \rightarrow S_{i-j}$, where $j \geq 1$.*

PROOF. Since σ is not cellular, there is a gap g that is not homeomorphic to an open disk. Then the gap g contains a closed curve c that is not contractible in g . There are two cases.

First we suppose that the closed curve c separates the surface S_i into two surfaces-with-boundary, $S_j - \text{int}(D)$ and $S_{i-j} - \text{int}(D')$, where D and D' are closed disks. If the woven image $\sigma(\mathcal{C})$ intersects both $S_j - \text{int}(D)$ and $S_{i-j} - \text{int}(D')$, then the weaving σ is separable into two disjoint non-empty weavings, one on S_j and the other on S_{i-j} . Otherwise, if $\sigma(\mathcal{C}) \cap S_j = \emptyset$ (a similar analysis applies when $\sigma(\mathcal{C}) \cap S_{i-j} = \emptyset$), then $S_j - \text{int}(D)$ cannot be homeomorphic to an open disk – lest the closed curve c be contractible in the gap g , which is contrary to supposition. Therefore, the image of the weaving σ is entirely contained in S_{i-j} , and S_j is an orientable surface of positive genus. Thus, the weaving σ is interpretable as an immersion from the circuit collection \mathcal{C} into the surface S_{i-j} , with $j \geq 1$.

Alternatively, if the closed curve c is non-separating on the surface S_i , then cut the surface S_i along c , and fill the two resulting holes with open disks, to obtain the surface S_{i-1} . The weaving σ is now interpretable as an immersion of the circuit collection \mathcal{C} on the surface S_{i-1} . \square

To understand which extended rotation systems of a graph G induce cellular weavings, we start with Lemma 3.2 and Corollary 3.3, which can be easily verified. It asserts that a weaving induced by an arbitrary ERS of a graph can also be induced by a **tri-valued rotation system** (abbr. **TRS**) in which only 0-twisted, 1^+ -twisted, and 1^- -twisted edges are allowed, if the graph G is replaced by a subdivision of itself.

Lemma 3.2 Let $\sigma : \mathcal{C} \rightarrow S_i$ be a weaving induced by an ERS ρ_G of a graph G , and let e be an edge in ρ_G that is k^+ -twisted (resp. k^- -twisted) with $k > 1$. Then the weaving σ is also induced by the ERS that is obtained from ρ_G by replacing the edge e with a path of k^+ -twisted (resp. 1^- -twisted) edges.

Corollary 3.3 Let $\sigma : \mathcal{C} \rightarrow S_i$ be a weaving induced by an ERS ρ_G of a graph G . Then the weaving σ is also induced by a tri-valued rotation system.

3.1 Medial graphs

Two gaps in a weaving $\sigma : \mathcal{C} \rightarrow S_i$ are **adjacent** if they share a common strand segment. The weaving σ is **2-colorable** if its gaps can be colored with two colors, such that no two adjacent gaps are assigned the same color.

Figure 5(a) illustrates an imbedding $K_4 \rightarrow S_0$ induced by a pure rotation system on K_4 . Figure 5(b) is a redrawing of 5(a) so that the strands of the weaving are pulled out of the corners. In the ERS of that figure, every edge of the graph K_4 is twisted. The weaving induced by the Strand-Tracing Algorithm has three strands, which are colored blue, green, and red. There are eight gaps, four of which, called **vertex-gaps**, are neighborhoods of the four vertices, and four of which, called **face-gaps**, lie in the interiors of the four faces of the pure rotation system. We observe the following two properties.

- Each of the gaps is a 2-cell.
- The adjacencies of each vertex-gap are only to face-gaps, and each face-gap is adjacent only to vertex-gaps.

Theorem 3.6 establishes that these two properties always hold when all the edges are twisted. Introducing the concept of *medial graph* paves the way to a short proof.

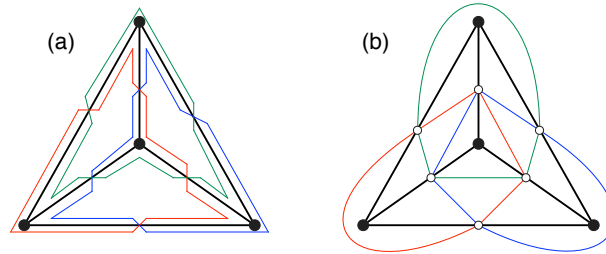


Figure 5: (a) The graph K_4 with an ERS and the induced weaving.
(b) A multi-color medial graph for the imbedding $K_4 \rightarrow S_0$.

Let $G \rightarrow S_i$ be a cellular imbedding. The **medial graph** is constructed (e.g., see [8]) according to Algorithm 2. We recognize the white vertices and the colored edges in Figure 5(b) as the medial graph for the given imbedding $G \rightarrow S_0$.

Proposition 3.4 (see Theorem 2.1 of [8]) Let $G \rightarrow S_i$ be an imbedding of a 4-regular graph whose faces can be properly 2-colored. Then $G \rightarrow S_i$ is the medial graph imbedding for a unique dual pair of graph imbeddings in S_i .

An ERS for a graph is **simply-twisted** if every edge is either 1^+ -twisted or 1^- -twisted.

Proposition 3.5 Let ρ_G be a simply-twisted rotation system, such that the corresponding pure rotation system induces the graph imbedding $G \rightarrow S_i$, and let σ be the induced weaving. Then the σ -imbedding $\iota_\sigma : G_\sigma \rightarrow S_i$ is equivalent to the imbedding of the medial graph for $G \rightarrow S_i$.

Algorithm MedialGraph(ρ_G^0)Input: a pure rotation system ρ_G^0 for a graph G .

Output: an imbedding of the corresponding medial graph.

- (S0) Use an applied face-tracing (see [15]) on the pure rotation system ρ_G^0 to construct an imbedding $G \rightarrow S_i$.
- (S1) For each edge $e \in E_G$,
 Install a medial vertex w_e in the interior of e —
 this vertex is usually drawn at or near the middle of e .
- (S2) For each corner (v, e, e') of each face f of the imbedding $G \rightarrow S_i$,
 Insert an edge $[w_e, w_{e'}]$ within the face f .
- (S3) For each edge $e = [u, v] \in E_G$, we suppose that the corners (u, e', e) and (v, e, e'') lie on one side of e and that the corners (v, d', e) and (u, e, d'') lie on the other side.
 The induced rotation at the medial vertex w_e is $w_e \cdot w_{e'} \cdot w_{e''} \cdot w_{d'} \cdot w_{d''}$

Algorithm 2: The medial-graph algorithm.

Theorem 3.6 *A 2-colorable weaving $\sigma : \mathcal{C} \rightarrow S_i$ is cellular if and only if it is inducible from a simply-twisted rotation system of a graph.*

PROOF. Let $\iota_\sigma : G_\sigma \rightarrow S_i$ be the induced 2-colorable, cellular σ -imbedding. The graph G_σ is clearly 4-regular, and a facial 2-coloring is inherited from the weaving $\sigma : \mathcal{C} \rightarrow S_i$. By Proposition 3.4, there is a graph imbedding $G \rightarrow S_i$ for which $\iota_\sigma : G_\sigma \rightarrow S_i$ is the medial imbedding. Take ρ_G to be the ERS whose pure rotation system corresponds to the imbedding $G \rightarrow S_i$, with every edge either 1^+ -twisted or 1^- -twisted, so as to reproduce the overcrossings and undercrossings of $\sigma : \mathcal{C} \rightarrow S_i$.

Conversely, let ρ_G be a simply-twisted rotation system of a graph G . The medial graph of the imbedding $G \rightarrow S_i$ induced by the corresponding pure rotation system is cellular. We observe that some faces of the medial graph imbedding lie within a face of the imbedding $G \rightarrow S_i$, and that each of the others contains a vertex of G . If the former are colored with one color and the latter with another color, then the result is a 2-coloring of the map of the medial imbedding. \square

3.2 Topological edge-contraction

Let ρ_0 be a pure rotation system of a graph G on a surface S_i and let e be an edge of G . **Contracting the edge e (topologically) in (the imbedding induced by) the rotation system ρ_0** means to continuously shrink the edge e on the surface S until its two ends meet. Any self-loops or multiple edges that result from this are retained in topological contractions, in which respect they differ from the “combinatorial contractions” that occur in the theory of simple graphs. Let $e = [u, v]$, and let the endpoints u and v in $\rho_0(G)$ have the following rotations, respectively:

$$u : u_1, \dots, u_{i-1}, v, u_{i+1}, \dots, u_s; \quad v : v_1, \dots, v_{j-1}, u, v_{j+1}, \dots, v_t. \quad (1)$$

Contracting the edge in ρ_0 replaces the two vertices u and v with a new vertex w whose rotation is

$$w : u_1, \dots, u_{i-1}, v_{j+1}, \dots, v_t, v_1, \dots, v_{j-1}, u_{i+1}, \dots, u_s. \quad (2)$$

It is well-known in topological graph theory that contracting an untwisted edge that is not a self-loop in an (orientable or non-orientable) imbedding does not change the imbedding surface. We can generalize edge contraction to extended rotation systems of a graph.

Definition Let ρ be an ERS of a graph G consisting of a pure rotation system ρ_0 and an edge-twist assignment. Let e be an edge in G . Then *contracting the edge e in the ERS ρ* results in a new ERS, whose pure rotation system is obtained by contracting the edge e in ρ_0 , with edge-twist assignments on all other edges identical to that in $\rho(G)$.

Theorem 3.7 *Let ρ be an ERS of a graph G , and let ρ' be the ERS obtained by contracting a 0-twisted edge e in ρ , where e is not a self-loop. Then the ERS ρ and the ERS ρ' induce equivalent weavings, on the same surface.*

PROOF. Let σ be the weaving induced by the ERS ρ . Since the edge e is 0-twisted, it is easy to verify that the edge e in $\rho(G)$ is entirely contained in a single vertex-gap in the weaving σ . Contracting the edge e in $\rho(G)$ contracts a line segment (corresponding to the edge e) in that vertex-gap. This changes neither the surface topology nor the gap structure in σ . Therefore, the ERS $\rho'(G')$ induces equivalent weavings, on the same surface. \square

Let E_1 be a subset of edges of a graph G . Let $G(E_1)$ denote the subgraph of G whose vertex set consists of the end-vertices of the edges in E_1 and whose edge set is E_1 .

Corollary 3.8 *Let ρ be an ERS, and let ρ' be an ERS obtained by contracting a set E_1 of 0-twisted edges in $\rho(G)$, such that the subgraph $G(E_1)$ is acyclic. Then the ERS ρ and the ERS ρ' induce equivalent weavings, on the same surface.*

Combining Corollary 3.8 and Theorem 3.6, we obtain

Theorem 3.9 *A 2-colorable weaving is cellular if and only if it is inducible by an ERS ρ of a graph G in which the subgraph $G(E_1)$ contains no cycles, where E_1 is the set of all 0-twisted edges in ρ .*

4 Normal Weaving

Cellular weaving requires that every gap is homeomorphic to an open disk, which is sometimes too restrictive. Indeed, it is not rare that an artistic weaving pattern consists of several disjoint and unlinked pieces (in which case the σ -graph is not connected), so that the weaving cannot be cellular. Figure 6 gives some examples of such weaving patterns. In this section, we characterize a more general class of weavings, called *normal weavings*, as inducible from extended graph rotation systems. For instance, this characterization implies that all the weavings in Figure 6 are inducible from extended graph rotation systems.



Figure 6: Examples of non-cellular weaving patterns (from [11])

We recall that a weaving is *2-colorable* if its gaps can be colored with 2 colors such that no two adjacent gaps have the same color. Such a coloring is called a *2-coloring of the weaving*.

Definition A weaving is *normal* if it has a 2-coloring in which every gap in one of the two colors is homeomorphic to an open disk. It is clear that a cellular weaving is a special case of a normal weaving.

Theorem 4.1 *Let ρ_G be an ERS of a graph G . Then the induced weaving σ is normal.*

PROOF. The proof is somewhat similar to one direction of the proof of Theorem 3.6. The graph G continues to be taken to be connected, but we now allow some 0-twisting in the ERS ρ_G , as well as 1^+ - or 1^- -twisting. Invoking Lemma 3.2 once again enables us to ignore higher multiplicity twisting.

We suppose that the pure rotation system ρ_G^0 imbeds the graph G on an orientable surface S_i , so that the weaving σ induced by ρ_G is a weaving on the surface S_i . We construct the weaving $\sigma : \mathcal{C} \rightarrow S_i$ with the algorithm **NormalWeave** (Algorithm 3). Figure 7 illustrates why the weaving σ is normal.

NormalWeave (ρ_G)
Input: an ERS ρ_G for a graph G .
Output: a normal weaving on the surface induced by the ERS ρ_G .

(S0) Use face-tracing (see [15]) to construct the orientable imbedding $G \rightarrow S$ based on the pure rotation system ρ_G^0 .
(S1) For each oriented edge \hat{e} induced by an edge e on an fb-walk f in ρ_G^0 :
(S1.1) if e is 1^+ - or 1^- -twisted, then place a crossing $x_{\hat{e}}$ at the middle of e — this crossing should preserve the crossing-sense of ρ_G ;
(S1.2) if e is 0-twisted, then place a point $x_{\hat{e}}$ in the face f near the middle of e .
\\ Thus, if e is 1^+ - or 1^- -twisted, then for the two oriented edges \hat{e} and \hat{e}' induced by e ,
\\ then we have $x_{\hat{e}} = x_{\hat{e}'}$.
(S2) For every pair of oriented edges \hat{e}_1 and \hat{e}_2 that are consecutive along the fb-walk f in ρ_G^0 , insert an edge $[x_{\hat{e}_1}, x_{\hat{e}_2}]$ within the face f .
(S3) Remove all vertices and edges that are in the original graph G ; and
(S4) If a vertex $x_{\hat{e}}$ has degree 2, then smooth it.

Algorithm 3: The normal weaving algorithm.

To see why such a weaving has a 2-coloring, we consider how it evolves from the 2-colorable weaving σ^0 (illustrated with thin red lines in Figure 7(a)) associated with its pure rotation system ρ_G^0 . In the weaving σ^0 , there is one vertex gap, which amounts to a thickening of the entire graph. Since ρ_G^0 induces a cellular graph imbedding, all the face-gaps are 2-cells. Twisting an edge may cause some minor reshaping of face-gaps, but it does not merge them, affect their cellularity, or cause them to become adjacent to other face-gaps. Twisting an edge may split a vertex-gap into two vertex-gaps or change the connectivity of a vertex-gap, but it does not cause two vertex-gaps to become adjacent. Accordingly, the output of Algorithm 3 is a normal weaving. \square

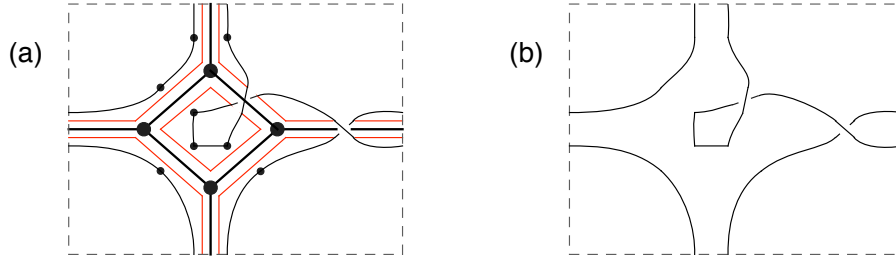


Figure 7: (a) Incipient induced weaving for an ERS, after Steps (S0), (S1), and (S2).
(b) Induced weaving, after Steps (S3) and (S4).

Proving the converse of Theorem 4.1 is more complicated.

The graph with one vertex and ℓ self-loops is called the *bouquet* of ℓ self-loops and denoted B_ℓ .

Theorem 4.2 *Let $\sigma : \mathcal{C} \rightarrow S_i$ be a normal weaving on a surface S_i . Then there is a graph G and an ERS ρ_G that induces σ .*

PROOF. We bipartition the gaps of the weaving $\sigma : \mathcal{C} \rightarrow S_i$ into F-gaps and V-gaps, such that no two gaps in the same group are adjacent, and so that every F-gap is homeomorphic to an open disk. (F-gaps and V-gaps will turn out to be face-gaps and vertex-gaps, respectively.)

The boundary-restored compactification of each V-gap m is a compact surface of some genus g with some number $k \geq 1$ of boundary components, each of which corresponds to one of the fb-walks of the imbedding $\iota_\sigma : G_\sigma \rightarrow S_i$ of the graph of the weaving $\sigma : \mathcal{C} \rightarrow S_i$. (All of the boundary components of a V-gap are missing.) The boundary-restored compactification $brc(m)$ of the surface m is homeomorphic (see [22]) to the result of pairing the sides of a $4g$ -sided flat polygon with k disjoint holes in its interior, so that the image of the polygon boundary is homeomorphic to B_{2g} . Accordingly, we can imbed the bouquet B_{2g} in the interior of the surface m so that every region is planar.

When $g = 0$, this means that we have placed the trivial graph B_0 in the interior of m . We conceptualize the “degenerate” 0-sided polygon with one vertex as the “flat polygon” for $brc(m)$.

We now add $k - 1$ more self-loops to this bouquet, each drawn so that it begins and ends at a corner of the flat polygon, so that there is a single hole in each region. The edges in the graph B_{2g+k-1} are called “dividing edges.” See Figure 8(a) for two representations of a gap with genus $g = 2$ and $k = 2$ holes.

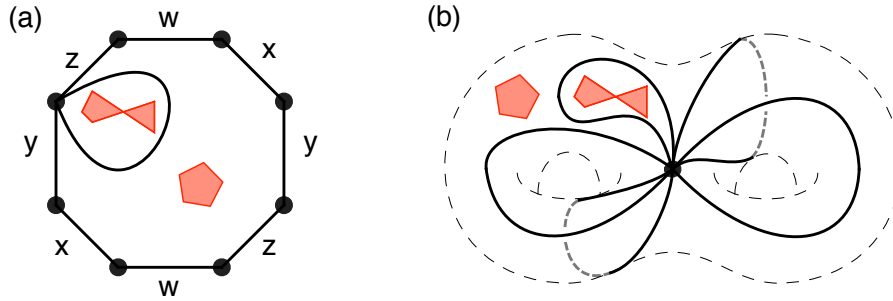


Figure 8: Two representations of a gap of genus 2 with two holes.

- (a) An 8-sided polygon with two (red) holes.
- (b) The corresponding imbedding of the bouquet B_5 in a two-holed surface of genus 2.

Our immediate task is construction of the graph G to be used for inducing the given normal weaving σ . We start with a single face f of the imbedding $\iota : B_{2g+k-1} \rightarrow m$, which contains exactly one hole. The boundary of that hole is a simple cycle in the compact surface $brc(m)$. We emphasize here that all of the boundary components of a gap are missing. Thus, when two F-gaps that are neighbors of a given V-gap meet each other at a vertex, the result of deleting the union of the boundaries of the two F-gaps is a single hole in the gap m , which we may regard as polygonal, with each side of the polygon corresponding to an edge of the graph G_σ . Figure 9(a) illustrates the face inside the monogon of the imbedding of B_5 in Figure 8(a). We observe that the vertex at which two F-faces meet has been virtually “pulled apart”, which is how it seems from the perspective of the V-gap.

Now choose any corner c of face f , and draw a set of internally disjoint simple curves on face f from the corner c to the corners of the polygonal hole inside face f , one to each polygon corner, as in Figure 9(b). These curves are called “semi-edges”, and the resulting faces within face f are called “semi-faces”. (It will soon be clear why we name these objects so.) We construct semi-edges similarly in every face of the gap m and we call the result G_m . We repeat this construction in every face of every V-gap. We consider the union

$$\bigcup_{\text{all V-gaps } m} G_m$$

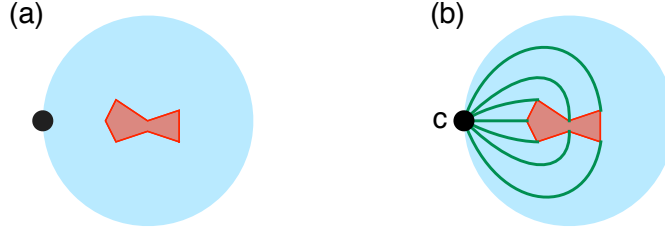


Figure 9: (a) Virtual merging of a 3-sided hole and a 4-sided hole into a 7-sided hole.
 (b) Seven “semi-edges” from the corner c to the seven corners of the polygonal hole, and the seven resulting “semi-faces”.

over all V-gaps in the weaving $\sigma : \mathcal{C} \rightarrow S_i$. Since each crossing in σ is on exactly two V-gap corners (which may belong to the same gap), there are exactly two semi-edges meeting at that crossing. We weld two such semi-edges into a single edge, which we call a “connecting edge”. We denote the resulting graph by G and its imbedding in S_i by $\iota : G \rightarrow S_i$. We will show that an ERS of the graph G based on the imbedding $\iota : G \rightarrow S_i$ induces the weaving σ .

Each face x of the imbedding $\iota : G \rightarrow S_i$ is the union of a single s -sided polygonal F-gap of the weaving $\sigma : \mathcal{C} \rightarrow S_i$ with the s semi-faces that meet its s sides, obtainable by pasting each of the semi-faces to the F-gap across one of the sides of the F-gap. Since the F-gap is cellular, and since each of the semi-faces is cellular, it follows that the face x is cellular. Accordingly, the imbedding $\iota : G \rightarrow S_i$ is cellular. This implies that the graph G is connected.

Let ρ_G^0 be the pure rotation system of the connected graph G corresponding to the cellular imbedding $\iota : G \rightarrow S_i$. Let ρ_G be the ERS of the graph G that consists of the pure rotation system ρ_G^0 and the edge-twist assignment such that all dividing edges in G are 0-twisted and the connecting edges in G are 1^+ -twisted or 1^- -twisted, so as to be consistent with the weaving σ , as illustrated in Figure 10(a,b).



Figure 10: Twisting a connecting edge (green) to be consistent with the given weaving (red).

Let σ_G be the weaving on the surface S_i that is induced by the ERS ρ_G . By construction, the weaving σ_G has a crossing wherever the given weaving σ has a crossing, and only where σ has a crossing. This implies a bijection between the set of strands of σ and the set of strands of σ_G . Moreover, each crossing of σ_G is of the same type as the corresponding crossing of σ . It follows that the two weavings are equivalent. \square

Theorem 4.1 and Theorem 4.2 combine into the following:

Corollary 4.3 *A weaving σ is inducible by an ERS of a graph if and only if σ is a normal weaving.*

5 Alternating Weaving and Plane Weaving

In this section, we characterize two special weaving classes, *alternating weavings* on general surfaces and *plane weavings*, in terms of extended rotation systems of graphs,

5.1 Alternating weaving

An *alternating weaving* is a weaving $\sigma : \mathcal{C} \rightarrow S_i$ such that, when traversing the image $\sigma(c)$ of any circuit $c \in \mathcal{C}$, one alternately crosses *over* and *under*. Alternating weaving, which is also called *plain weaving* in weaving literature, has been among the most widely used weaving patterns in practice [7]. The first three objects in Figure 3 are examples of alternating weaving.

An edge in an ERS ρ of a graph G is *positively twisted* (resp. *negatively twisted*) if it is k^+ -twisted (resp. k^- -twisted) for some integer $k > 0$. An ERS of a graph is *uni-direction-twisted* if either none of its edges are positively twisted or none of its edges are negatively twisted. Theorem 5.1 is known. For completeness, we give a proof here, which is also useful for our proof of the theorem immediately after.

Theorem 5.1 [7] *Let ρ be a uni-direction-twisted ERS of a graph G . Then ρ induces an alternating weaving.*

PROOF. The corresponding pure rotation system ρ_0 induces a cellular imbedding $G \rightarrow S_i$ for some genus i . We shall suppose that the ERS ρ is positively twisted. By Lemma 3.2, we can assume without loss of generality that each edge in $\rho(G)$ is either 0-twisted or 1^+ -twisted. Let σ be the weaving on the surface S_i that is induced by ρ . If the weaving σ contains no crossings, then, by definition, σ is an alternating weaving.

Thus, suppose that the weaving σ has crossings, and suppose that the strand $s = \sigma(c)$ goes “under” at a crossing x . Then the crossing x is induced by a 1^+ -twisted edge e in $\rho(G)$. Accordingly, as one traverses the edge e on the surface S_i , the strand s must start at one’s right, pass through the crossing x , and then continue on one’s left along the edge (see Figure 4(b)). After the crossing x , the strand s continues its traversal along an fb-walk of the pure rotation system $\rho_0(G)$, while staying to one’s left on each traversed edge, until it encounters the next crossing x' . Let the crossing x' be induced by a 1^+ -twisted edge e' (note that x' could be x and that e' could be e). At the crossing x' , the strand s then crosses from the left side of the edge e' to the right side. Again because e' is 1^+ -twisted, the strand s must go “over” at the crossing x' , as shown in Figure 11, where the strand s is colored blue.

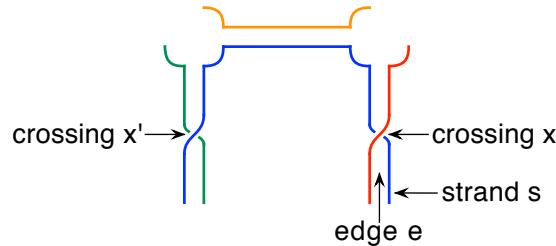


Figure 11: The alternating weaving induced by a uni-direction-twisted rotation system.

Similarly, if the strand s emerges from a crossing where it goes “over”, then the strand must go “under” at the next crossing. This proves that the weaving σ induced by $\rho(G)$ is an alternating weaving. The case where no edges in $\rho(G)$ are positively twisted can be proved similarly. \square

We recall that the σ -graph uses the crossings of σ as vertices and the strand segments in σ as edges. For a normal weaving σ with a connected σ -graph, Theorem 5.1 has a converse.

Theorem 5.2 *Let $\sigma : \mathcal{C} \rightarrow S_i$ be a normal weaving with a connected σ -graph. Then σ is an alternating weaving if and only if it is induced by a uni-direction twisted ERS of a graph.*

PROOF. If the weaving σ is induced by a uni-direction-twisted ERS of a graph, then by Theorem 5.1, σ is an alternating weaving.

Now suppose, conversely, that σ is a normal, alternating weaving. By Theorem 4.3, the weaving σ is induced by an ERS ρ of a graph G . By Lemma 3.2, we can assume without loss of generality that each edge is 0-twisted, 1^+ -twisted, or 1^- -twisted in ρ . If the ERS ρ is not uni-direction-twisted, then there must be edges $e, e' \in E_G$, such that e is 1^+ -twisted and e' is 1^- -twisted in ρ .

Let x and x' be the crossings in σ that are induced by the edges e and e' , respectively. Since the σ -graph is connected, there is a sequence of strand segments (corresponding to a path in the σ -graph):

$$s_1, s_2, \dots, s_q$$

such that

- strand segment s_1 starts from crossing x ;
- strand segment s_q ends at crossing x' ;
- for $j = 1, \dots, q - 1$, strand segment s_j and strand segment s_{j+1} share a common crossing.

Since x is induced by the 1^+ -twisted edge e and x' is induced by the 1^- -twisted edge e' , there must be a strand segment s_j in this sequence such that one crossing of s_j is induced by a 1^+ -twisted edge and the other crossing of s_j is induced by a 1^- -twisted edge. Now by an analysis similar to that in the proof of Theorem 5.1 (see Figure 11, where we showed that if both crossings of a strand segment are induced by two edges of the same twist type, then the strand segment proceeds alternately), we can verify that the strand segment s_j either goes over at both its crossings or goes under at both its crossings. This contradicts the premise that the weaving σ is alternating. \square

Combining Theorem 5.1 and Theorem 4.3, we also have the following result.

Theorem 5.3 *Any normal weaving $\sigma : \mathcal{C} \rightarrow S_i$ can be converted into an alternating weaving by appropriately changing some edge-crossing types.*

PROOF. By Theorem 4.3, the weaving σ is induced by an ERS ρ of a graph G . Let ρ' be the ERS of graph G obtained from ρ by changing the twist type of each k^- -twisted edge, where $k > 0$, to k^+ -twisted. Then the ERS ρ' is uni-direction-twisted. By Theorem 5.1, the weaving σ' induced by ρ' is alternating. It is easy to see that the σ -imbedding and the σ' -imbedding are identical on the surface S_i . (More precisely, there is an autohomeomorphism on the surface S_i that maps the image of the σ -imbedding $\iota_\sigma : G_\sigma \rightarrow S_i$ to the image of the σ' -imbedding $\iota_{\sigma'} : G_{\sigma'} \rightarrow S_i$.) Therefore, the normal weaving σ can be converted into the alternating weaving σ' by properly changing some crossing types. \square

5.2 Plane weaving

In this subsection, we consider arbitrary weavings on the plane \mathbb{R}^2 (or equivalently, on the sphere). Most weavings in the weaving literature are on the plane. All the weaving patterns in Figure 6 are on the plane. Most Celtic knot patterns [9] are weavings on the plane. The second and the third images in Figure 3 are woven on the sphere.

We first consider the weavings σ on the plane whose σ -graph is connected. Recall that an ERS of a graph is simply-twisted if every edge of the graph is either 1^+ -twisted or 1^- -twisted.

Theorem 5.4 *Let $\sigma : \mathcal{C} \rightarrow \mathbb{R}^2$ be a plane weaving whose σ -graph G_σ is connected. Then σ is a cellular weaving, and it is inducible by a simply-twisted ERS of a planar graph.*

PROOF. Each vertex of the graph G_σ represents a crossing of the weaving σ and has degree 4. Therefore, the σ -imbedding $\iota_\sigma : G_\sigma \rightarrow \mathbb{R}^2$ induces a plane map in which every vertex is 4-valent. By Kempe's two-color map theorem [24], such a map is 2-colorable. Accordingly, the weaving σ is 2-colorable. Moreover, the σ -imbedding $\iota(G_\sigma)$ is cellular, because a planar imbedding of any connected graph is cellular. Thus, by Theorem 3.6, the weaving σ is inducible by a simply-twisted ERS of a planar graph. \square

When a weaving σ is cellular on the plane, the induced graph G_σ is connected. Then the weaving σ corresponds to a simply-twisted ERS ρ , i.e., of a pure rotation system ρ_0 and an edge-twist assignment. Such a weaving σ has a unique unbounded “outer gap” and a collection of bounded “inner gaps”. The outer gap of the weaving σ is a face-gap corresponding to the “infinite” face of the induced imbedding $\iota_\sigma : G_\sigma \rightarrow \mathbb{R}^2$.

If we allow the σ -graph to be non-connected, then the corresponding weaving on the plane need not be normal. We can construct such a weaving, starting with an arbitrary weaving σ on the plane. We insert two separated small weavings σ_1 and σ_2 into two adjacent gaps g_1 and g_2 , respectively, in σ , so that the images of the weavings σ , σ_1 , and σ_2 are pairwise disjoint on the plane. To see that the resulting weaving $\sigma' = \sigma + \sigma_1 + \sigma_2$ is not normal, let $\bar{\sigma}_1$ and $\bar{\sigma}_2$ represent the corresponding weavings plus all their inner gaps. Then the two gaps $g_1 - \bar{\sigma}_1$ and $g_2 - \bar{\sigma}_2$ are adjacent in σ' but neither is homeomorphic to an open disk.

Accordingly, to represent all weavings on the plane, we need to enhance the structures of extended rotation systems of a graph. We consider a plane weaving σ whose σ -graph has connected components C_1, C_2, \dots, C_h , with $h > 1$, corresponding to planar “sub-weavings” $\sigma_1, \sigma_2, \dots, \sigma_h$ of σ , each of whose induced graphs G_{σ_j} is connected. We say that a sub-weaving σ_i is a **child** of another sub-weaving σ_j if the image of σ_i is entirely contained in an inner gap g of σ_j , and if there is no intermediate sub-weaving σ_t whose image of also lies within gap g , such that the image of σ_i lies within an inner gap of σ_t . Note that a sub-weaving σ_i of σ either is not directly contained in any other sub-weaving, or is directly contained in a unique sub-weaving σ_j .

This parent-child relationship carries over to the corresponding simply-twisted extended rotation systems. The structure of the weaving σ can be represented by a **tree of rotation systems**, denoted T_σ , where a virtual empty weaving σ_0 is chosen as the root. We label the edges of the tree with information to indicate into which face-gap or vertex-gap a given child is to be contained. This establishes the following theorem:

Theorem 5.5 *A weaving is on the plane if and only if it can be specified by a tree of rotation systems in which each node, except the root, is a simply-twisted ERS that induces a weaving on the plane.*

For instance, each of the weaving patterns in Figure 6 can be specified by a tree of rotation systems.

6 Subdivided Imbeddings and Dual Imbeddings

In this section, we demonstrate how extended rotation systems of graphs provide a practical model for weavings on general topological surfaces. In particular, we establish a correspondence between two operations on weavings that are well-established in the computer graphics community, the Catmull-Clark subdivision and the Doo-Sabin subdivision, with topological operations on extended rotation systems of a graph. Under this straightforward correspondence, these two operations can be readily implemented by a graphics system based on extended rotation systems. For describing the correspondence with the Catmull-Clark operation, we introduce a new *doubling operation* on weavings.

6.1 Catmull-Clark subdivisions

Given a cellular imbedding $\iota : G \rightarrow S_i$ of a graph G , as in Figure 12(a), with induced pure rotation system ρ_0 , the **Catmull-Clark³ subdivision operation** [10] builds a new graph G^{cc} and its imbedding $\iota^{cc} : G^{cc} \rightarrow S_i$ in that same surface, with induced pure rotations system ρ_0^{cc} as follows:

³We note that the Catmull-Clark algorithm is used in computer graphics to create smooth subdivided surfaces. In that context, the geometric locations of the new (and old) vertices are carefully considered. Our present discussion focuses on the topological properties of the resulting imbedding.

- (1) into the interior of each edge $e \in E_G$, insert a vertex w_e , as in Figure 12(b);
- (2) into the interior of each face f in $\rho_0(G)$, insert a vertex w_f , as in Figure 12(c);
- (3) for each face f and each edge e on the boundary of the face f in $\rho_0(G)$, add an edge $[w_f, w_e]$, as in Figure 12(d), which also depicts the induced pure rotation system on G^{cc} ;
- (4) if the oriented fb-walk for face f is d_1, d_2, \dots, d_m , then the induced rotation at the vertex w_f is $[w_f, w_{e_1}], [w_f, w_{e_2}], \dots, [w_f, w_{e_m}]$; and
- (5) if edge $e = [u, v]$ is incident on faces f and f' , and if the corner (u, x, e) of face f immediately precedes the corner (v, e, y) , as the fb-walk traverses edge e , then the induced rotation at the vertex w_e is $[w_e, u], [w_e, w_f], [w_e, v], [w_e, w_{f'}]$.

Topologists will recognize that the graph G^{cc} is a subgraph of the 1-skeleton of the barycentric subdivision of the 2-complex specified by the imbedding $\iota : G \rightarrow S_i$.

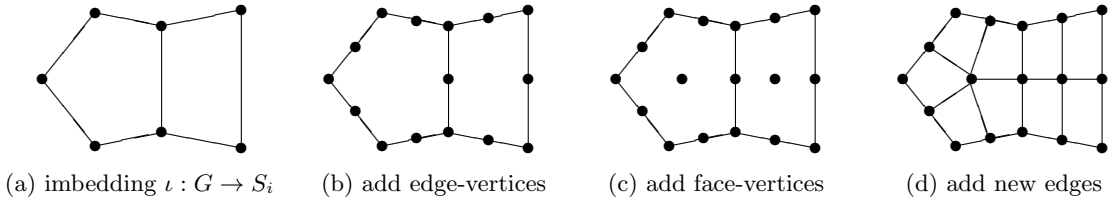


Figure 12: Catmull-Clark subdivision

6.2 The doubling operation on weavings

We now examine how a Catmull-Clark subdivision is realized in an ERS of a graph and a consequence on the induced weaving. For this, we first introduce a new operation on weaving.

Definition Let c be a strand in a weaving σ in a surface S_i . We **double the strand** c in the weaving σ as follows:

- (1) we replace strand c by two parallel and closely positioned strands c_1 and c_2 , so that the only crossings of σ that are affected are those on the strand c ;
- (2) each crossing of strand c with itself or with any other strand c' is replaced by two consecutive crossings on c or c' , one with c_1 and the other with c_2 ;
- (3) the crossing-types of the new crossings are left undetermined for the time being.

Definition Let σ be a weaving on a surface S_i . The result of doubling every strand is called a **doubling of the weaving** σ^2 . (We will focus on doublings that are alternating weavings.)

Figure 13 shows a twill and a possible doubling and redoubling, in which crossing-types were assigned so that the new weavings are twills. In a twill, each strand goes two over and two under, cyclically, with one shift between two adjacent strands.

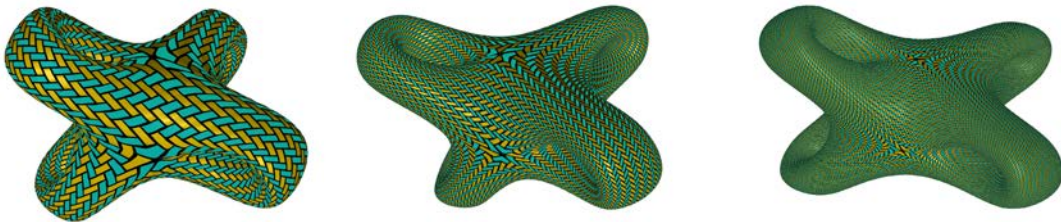


Figure 13: A weaving, doubled and redoubled.

Doubling a weaving creates a “refined” weaving on the same surface. Further importance of doubling will emerge in two subsequent papers [4, 5], where we see that the assignment of crossing types will allow us to construct different weaving patterns on a topological surface. An immediate indication of the utility of doubling is revealed by the following theorem.

Theorem 6.1 *Let σ be any weaving. Then a doubled weaving σ^2 is a normal weaving.*

PROOF. We recall that a weaving is normal if its gaps can be colored with two colors such that no two adjacent gaps are assigned with the same color and that all gaps in one of the colors are cellular. In a doubled weaving, every gap that corresponds to a crossing or face-gap of the original weaving can be colored blue, and every gap that corresponds to a former strand segment (from crossing to crossing) can be colored red, as illustrated in Figure 14. In this proper 2-coloring, every red region is cellular. \square

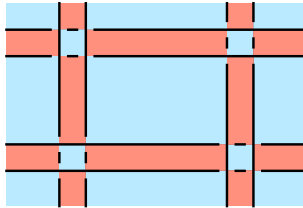


Figure 14: 2-coloring the gaps of a doubled weaving.

Remark 6.1 *We observe that Theorem 6.1 holds true for any weaving σ on any surface. In particular, the weaving σ need not be inducible by an ERS of a graph.*

The following theorem reveals how a Catmull-Clark subdivision can be realized by the weaving doubling operation.

Theorem 6.2 *Let ρ be a simply-twisted ERS of a connected graph G with pure rotation system ρ_0 and induced weaving σ , and let ρ^{cc} be any simply-twisted ERS of the graph G^{cc} whose pure rotation system ρ_0^{cc} is obtained by applying Catmull-Clark subdivision to ρ_0 . Then the weaving σ^{cc} induced by ρ^{cc} is obtainable by assigning appropriate crossing-types to a doubling of the weaving σ .*

PROOF. Figure 15 serves as an intuitive guide through the combinatorial details of the proof. The area of chief concern is highlighted in yellow.

Since the ERS ρ is simply-twisted, each edge of the graph G induces exactly one crossing, which we place at the middle of the edge. Consider three consecutive crossings along a strand c (shown in blue) of the weaving σ , say along three edges $e_1 = [v_1, v_2]$, $e_2 = [v_2, v_3]$, and $e_3 = [v_3, v_4]$, respectively. Therefore, in the pure rotation system ρ_0 , the triple (v_2, e_1, e_2) makes a corner of a face f , the triple (v_3, e_2, e_3) makes a face corner of a face f' , and edge e_2 is on the boundary of the faces f and f' . Figure 15 assumes, without loss of generality, that the strand c is on the right side of edge e_1 before it traverses that edge e_1 (along the direction of traversal).

Applying Catmull-Clark subdivision to the pure rotation system ρ_0 yields the pure rotation system ρ_0^{cc} , as shown in Figure 15(b), where new vertices w_f and $w_{f'}$ are inserted into faces f and f' , respectively; new vertices u_1 , u_2 , and u_3 are inserted at the middle of the edges e_1 , e_2 , and e_3 , respectively; and new edges $[w_f, u_1]$, $[w_f, u_2]$, $[w_{f'}, u_2]$, and $[w_{f'}, u_3]$ are added. The new vertices are shown as hollow circles and the new edges as thin line segments. To avoid cluttering the diagram, we have not transported labels from Figure 15(a).

Now consider a strand c' (thin blue) that starts at the right side of the edge $[v_1, u_1]$ in the weaving σ^{cc} induced by the ERS ρ^{cc} . Since the ERS ρ^{cc} is also simply-twisted, it is easy to verify, as shown in Figure 15(c), that the order in which the strand c' crosses edges of the subdivided graph G^{cc} is

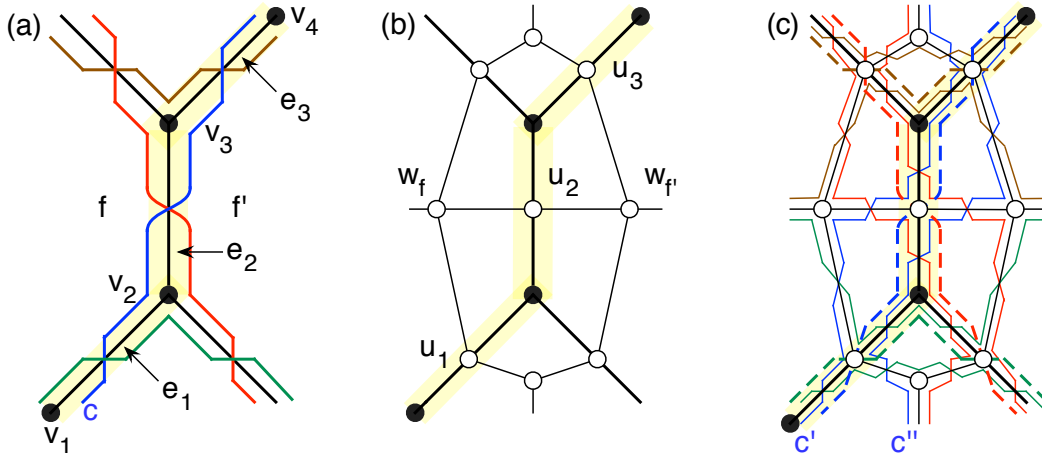


Figure 15: (a) The weaving strands induced by a simply-twisted ERS. (b) The Catmull-Clark subdivision of the imbedded graph that induces the weaving. (c) Doubling the strands.

$$[v_1, u_1], [u_1, w_f], [w_f, u_2], [u_2, v_3], [v_3, u_3]$$

Observe that this sequence of segments of the strand c' can be drawn in parallel with the part of the strand c (broken blue line) between the crossings on edges $[v_1, v_2]$ and $[v_3, v_4]$. Indeed, the entire strand c' can be drawn “in parallel” with the strand c on the surface, in the sense of deforming strand c' to strand c without passing through any edges of the initial graph G . This is because the crossing of c' on the edge $[v_3, u_3]$ repeats the configuration of its crossing on the edge $[v_1, u_1]$, relative to its relationship with strand c ; that is, it starts at the right side of the edge $[v_3, u_3]$. Thus, just as the strand c' lies parallel to the strand c in their course along edges e_1 and e_2 , it will also lie parallel to the strand c in their course along edge e_3 and whatever edge strand c traverses immediately after edge e_3 . This parallel course continues over the entire course of strands c and c' , until they both return to vertex v_1 . (The strand c has an even number of crossings because the surface of the weaving is orientable.)

Similarly, if we traverse the part of the strand c'' in the weaving σ^{cc} that starts at vertex u_1 from the right side of the edge $[u_1, v_2]$ in the imbedding of G^{cc} , we can show that the strand c'' can also be drawn in parallel with the strand c on the surface. Thus, the two parallel strands c' and c'' in the weaving σ^{cc} correspond to the result of doubling the strand c in the weaving σ . That there no strands other than c' and c'' in the weaving σ' follows from these simple facts:

1. the number of edges in the graph G^{cc} is exactly four times that in the graph G (see the edge $[v_2, v_3]$ in the middle figure of Figure 15);
2. the number of crossings in the weaving σ^{cc} is exactly four times that in the weaving σ (one on each edge of G^{cc}); and
3. each edge in a simply-twisted extended rotation system induces exactly one crossing.

This completes the proof that the weaving σ^{cc} can be obtained by doubling the weaving σ . □

6.3 Doo-Sabin subdivisions

The Doo-Sabin⁴ subdivision algorithm [12] was invented around the same time as the Catmull-Clark algorithm.

⁴Like the Catmull-Clark algorithm, the Doo-Sabin algorithm is used in computer graphics to create smooth subdivided surfaces.

Given a cellular imbedding $\iota : G \rightarrow S_i$, as in Figure 16(a), the Doo-Sabin operation on a graph imbedding $G \rightarrow S_i$ constructs a new graph G^{ds} and its imbedding $\iota^{ds} : G^{ds} \rightarrow S_i$ in the same imbedding surface as follows:

- (1) into the interior of each polygonal face f , we insert a cycle of the same length as the fb-walk of f , near to the fb-walk, as in Figure 16(b);
- (2) for each edge $e \in E_G$, join corresponding endpoints of the two parallel edges in the faces incident on e , as in Figure 16(c); and
- (3) discard the original graph G , as in Figure 16(d).

Topologists will recognize that the graph G^{cc} is a subgraph of the 1-skeleton of the barycentric subdivision of the 2-complex specified by the imbedding $\iota : G \rightarrow S_i$.

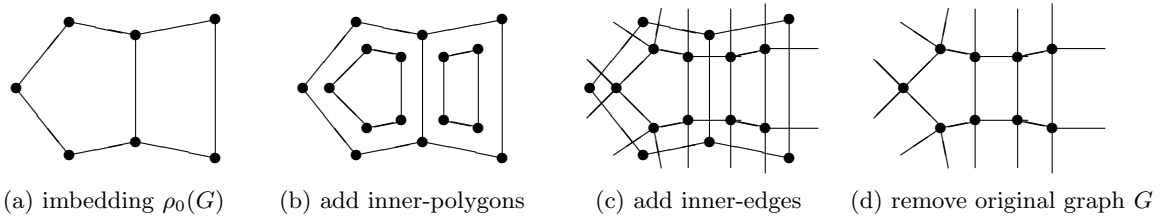


Figure 16: Doo-Sabin subdivision of a graph imbedding $G \rightarrow S_i$

6.4 Dual imbeddings

A pure rotation system ρ_0 on a connected graph G corresponds to a cellular imbedding $\iota : G \rightarrow S_i$ into an orientable surface. We recall that a **dual imbedding** $\iota^* : G^* \rightarrow S_i$ can be constructed as follows:

- (1) install a dual vertex w_f into the interior of each face f of the imbedding; and
- (2) through each edge e of the primal graph G , install an edge e^* that crosses edge e and joins the dual vertex w_f in the face on one side of e to the dual vertex $w_{f'}$ in the face on the other side of e . (Faces f and f' may be the same face).

The dual imbedding $\iota^* : G^* \rightarrow S_i$ induces a **dual pure rotation system** ρ_0^* on the dual graph G^* .

Theorem 6.3 *Let ρ and ρ^* be two simply-twisted extended rotation systems on graphs G and G^* , respectively, whose pure rotation systems ρ_0 and ρ_0^* are dual to each other. Let the edge-twisting value assigned to each dual edge $e^* \in E_{G^*}$ be opposite to the edge-twisting value assigned to the corresponding primal edge $e \in E_G$. Then the weavings σ and σ^* induced by ρ and ρ^* , respectively, are isomorphic.*

PROOF. We recall from Proposition 3.5 that the graph of the weaving induced by a simply-twisted extended rotation system is equivalent to the imbedding of the medial graph for the imbedding induced by the corresponding pure rotation system. Since a graph and its dual have the same medial graph imbedding, the theorem follows. \square

The following theorem can be easily verified. The duality is illustrated by Figure 17.

Theorem 6.4 *Let $\iota : G \rightarrow S_i$ be an imbedding of a connected graph G . Let $\iota^{cc} : G^{cc} \rightarrow S_i$ be the imbedding obtained by applying Catmull-Clark subdivision to $\iota : G \rightarrow S_i$, and let $\iota^{ds} : G^{ds} \rightarrow S_i$ be the imbedding obtained by applying Doo-Sabin subdivision to $\iota : G \rightarrow S_i$. Then $\iota^{cc} : G^{cc} \rightarrow S_i$ and $\iota^{ds} : G^{ds} \rightarrow S_i$ are dual imbeddings.*

Combining Theorem 6.3 and Theorem 6.4, and using Proposition 3.5, we obtain our final theorem:

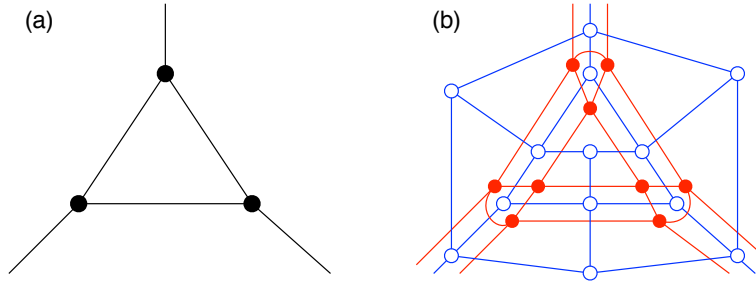


Figure 17: (a) A graph imbedding.
 (b) Superposition of the Clark-Catmull (blue) and Doo-Sabin (red) subdivisions.

Theorem 6.5 *Let ρ be a simply-twisted ERS of a connected graph G with pure rotation system ρ_0 , and let ρ^{ds} be a simply-twisted ERS of a graph G^{ds} whose pure rotation system ρ_0^{ds} is obtained from ρ_0 by applying Doo-Sabin subdivision. Then the weaving σ^{ds} induced by ρ^{ds} is obtainable by doubling the weaving σ induced by ρ and then assigning appropriate edge-twistings.*

6.5 Other topological operations on graph imbeddings

In topological graph theory, it is well known that each edge insertion, edge deletion, and edge twisting on a general rotation system of a graph either merges two faces into a single face or splits a single face into two faces. (See [2] for some recent updates.) The precise relationship between these elementary edge operations on an extended rotation system of a graph and the corresponding strand operations on the induced weaving can be easily derived, based on the *face-tracing algorithm* in topological graph theory [15] and the **strand-tracing algorithm** given here as Algorithm 1. We omit detailed discussion of these elementary operations. We focus on topological contraction, dualization, and subdivision.

7 Conclusion

Is every weaving induced by extended graph rotation systems? No. give examples.

We will do this after all other parts are done.

References

- [1] E. AKLEMAN, J. CHEN, AND J. L. GROSS, Paper-strip sculptures, *Proc. Shape Modeling International (SMI 2010)*, pp. 236–240, (2010).
- [2] E. AKLEMAN, J. CHEN, AND J. GROSS, Extended graph rotation systems as a model for cyclic weaving on orientable surfaces, *Submitted*, (2012).
- [3] E. AKLEMAN, J. CHEN, Y.-L. CHEN, Q. XING, AND J. L. GROSS, Cyclic twill-woven objects, *Computers & Graphics 35-3*, pp. 623–631, (2011).
- [4] E. AKLEMAN, J. CHEN, S. HU, AND J. L. GROSS, A topological theory of twill-woven images, *Manuscript in preparation*, (2012).
- [5] E. AKLEMAN, J. CHEN, S. HU, AND J. L. GROSS, Quad-pattern coverability in woven images, *Manuscript in preparation*, (2012).
- [6] E. AKLEMAN, J. CHEN, S. HU, AND J. L. GROSS, Weaving and permutation voltage graphs, *Manuscript in preparation*, (2012).

- [7] E. AKLEMAN, J. CHEN, Q. XING, AND J. L. GROSS, Cyclic plain-weaving with extended graph rotation systems, *ACM Transactions on Graphics 28-3* Article No. 78; (Proc. SIGGRAPH'2009), (2009).
- [8] D. ARCHDEACON, The medial graph and voltage-current duality, *Discrete Mathematics 104-2*, pp. 111–141, (1992).
- [9] G. BAIN, *Celtic Art: The Methods of Construction*, Dover Publications, Inc., New York, 1973.
- [10] E. CATMULL AND J. CLARK, Recursively generated B-spline surfaces on arbitrary topological meshes, *Computer Aided Design 10*, pp. 350–355, (1978).
- [11] Celtic knot - Wikipedia, the free encyclopedia, at http://en.wikipedia.org/wiki/Celtic_knot.
- [12] D. DOO AND M. SABIN, Behavior of recursive division surfaces near extraordinary points, *Computer Aided Design 10*, pp. 356–360, (1978).
- [13] J. EDMONDS, A combinatorial representation for polyhedral surfaces, *Notices American Mathematics Society 7*, p. 646, (1960).
- [14] J. L. GROSS AND T. W. TUCKER, A Celtic framework for knots and links, *Discrete & Computational Geometry 46-1*, pp. 86–99, (2011).
- [15] J. L. GROSS AND T. W. TUCKER, *Topological Graph Theory*, Wiley Interscience, New York, 1987.
- [16] J. L. GROSS AND J. YELLEN, *Graph Theory and Its Applications*, 2nd Ed., CRC Press, 2006.
- [17] B. GRÜNBAUM AND G. C. SHEPARD, Satins and twills: an introduction to the geometry of fabrics, *Mathematics Magazine 53-3*, pp. 139–161, (1980).
- [18] L. HEFFTER, Über das Problem der Nachbargebiete, *Math. Ann. 38*, pp. 477–508, (1891).
- [19] L. H. KAUFFMAN, *Formal Knot Theory*, Dover, New York, Original ed. Princeton University Press, 1983.
- [20] J. LEE, *Introduction to Topological Manifolds*, Springer, New York, 2011.
- [21] D. MACKENZIE, The Poincaré Conjecture — Proved, *Science 314*, pp. 1848–1849, (2006).
- [22] W. S. MASSEY, *Algebraic Topology: An Introduction* Harcourt, 1967.
- [23] Plain weave, *Encyclopaedia Britannica*, <http://www.britannica.com/EBchecked/topic/462734/plain-weave>
- [24] A. SOIFER, *The Mathematical Coloring Book*, Springer, New York, 2009.
- [25] C. THOMASSEN, The Jordan-Schonflies theorem and the classification of surfaces, *American Mathematical Monthly 99-2*, pp. 116–130, (1992).
- [26] O. VEBLEN, Theory on plane curves in non-metrical analysis situs, *Transactions of the American Mathematical Society 6-1*, pp. 83–98, (1905).